

## Replies to referee Report 1

We thank the reviewer for careful reading of the manuscript and several helpful suggestions that lead to an improvement of the text. Here we reproduce referee's comments in full and show our replies in blue font. Similarly, in the manuscript we use bold font to clearly denote the changed text.

Abstract, l2: 150km: tangent altitude? - please specify what this distance refers to.

Done

p3, l24: an "a" is missing before "series" and

p3, l26: "the" Martian atmosphere...

Both done

p4,l17: why was the altitude of 100km chosen for this comparison while the data discussed before refers to 115km? It would be more consistent to show this for the situation discussed before.

We added one new curve in left panel, and two in right panel of Figure 2 for the altitude of 120 km and  $\text{SZA}=69$  deg., which exactly correspond to the conditions of simulated spectra in Figure 1. We also modified the discussion of this figure in the text.

p4,l28: split infinitive "significantly better reproduces..." -> "reproduces ... significantly better compared to..."

Done

p4, sec 3.1: While the model does a very good job reproducing the observed feature, it seems that the ratio of the peaks is slightly shifted toward the left peak compared to the observed spectrum. Is there an obvious explanation for this (admittedly small) discrepancy? What is the estimated uncertainty in the modeled spectrum (e.g., arising from input data) also with respect to the absolute values of the derived radiances?

In order to clarify the "uncertainty in the modeled spectrum (e.g., arising from input data) also with respect to the absolute values of the derived radiances" let us consider left branches of spectra presented in Fig.1, which are mostly formed by the P-branches of 626 SH 4.3 bands considered. The latter are less influenced by a self-absorption in the cores compared to to the right branches of spectra associated with stronger R-branches of these bands.

Generally, the position of the peak for each of 27 single spectra used to obtain the measured mean distribution depends on (a) the temperature and pressure distributions in the atmosphere at the time of each particular scan, and (b) on the degree of self absorption of the radiation in the most intensive lines of branch core along the limb line-of-sight (LOS). This is also true for our simulated spectrum. For this case, the model temperature used in calculations is increasing from 136K at 120 km up to 225K at 150 km (and also higher for higher altitudes). This temperature increase causes the shift of the rotational distribution maximum along the LOS to higher  $j$  from  $j_{\text{max}}=11$  at 120 km to  $j_{\text{max}}=13$  at 150 km. The simulated spectrum is a resulting integral over the LOS, which also accounts for the self-absorption of lines.

It seems that one finally may find the model temperature/pressure distribution, which will provide

complete match of absolute values and shapes of measured (mean) and calculated (single) spectra, however, this was not the goal of this study.

p5, fig 1: assuming the figure will be smaller in the final layout it might be good to choose a different color or line width for the yellow line.

We increased the width of orange line.

p6, fig 2: typo in the x-axis label in the right panel see previous comment above: why is an altitude of 100km chosen here?

Typo is corrected, the curves for altitude of 120 km are added, see also reply above.

p6, l2: ... "the" first of these...

Corrected

p6/p7: The last paragraph of sec 3.2 requires some language improvements, especially with regard to missing articles and word order. Maybe some of the long sentences could be split.

We have rewritten the paragraph for clarity and easier reading.

p7, l20: ...does "an" excellent job...

Corrected

p7, l28: "...need of significant additional study..." - please rephrase this sentence to clarify.

Done

p8, l7: ...influence "the" main results...

Done

# Evidence of a significant rotational non-LTE effect in the CO<sub>2</sub> 4.3 μm PFS-MEX limb spectra

Alexander A. Kutepov<sup>1,2</sup>, Ladislav Rezac<sup>3</sup>, and Artem G. Feofilov<sup>4</sup>

<sup>1</sup>NASA Goddard Space Flight Center, Greenbelt, MD, USA

<sup>2</sup>The Catholic University of America, Washington, D.C., USA

<sup>3</sup>Max-Planck-Institut für Sonnensystemforschung, Justus-von-Liebig-Weg 3, 37077 Göttingen, Germany

<sup>4</sup>Laboratoire de Météorologie Dynamique, IPSL/CNRS, UMR8539, Ecole Polytechnique, France

*Correspondence to:* alexander.a.kutepov@nasa.gov

**Abstract.** Since January 2004, the planetary Fourier spectrometer (PFS) on board the Mars Express satellite has been recording near infrared limb spectra of high quality up to **the tangent altitudes**  $\approx 150$  km, with potential information on density and thermal structure of the upper **Martian** atmosphere. We present first results of our modeling of the PFS short wavelength channel (SWC) daytime limb spectra for the altitude region above 90 km. We applied a ro-vibrational non-LTE model based on the stellar astrophysics technique of accelerated lambda iteration (ALI) to solve the multi-species and multi-level CO<sub>2</sub> problem in the Martian atmosphere. We show that the long standing discrepancy between observed and calculated spectra in the cores and wings of 4.3 μm region is explained by the non-thermal rotational distribution of molecules in the upper vibrational states 10011 and 10012 of the CO<sub>2</sub> main isotope second hot (SH) bands above 90 km altitude. The redistribution of SH band intensities from band branch cores into their wings is caused (a) by intensive production of the CO<sub>2</sub> molecules in rotational states with  $j > 30$  due to the absorption of solar radiation in optically thin wings of 2.7 μm bands, and (b) by a short radiative life time of excited molecules, which is insufficient at altitudes above 90 km for collisions to maintain rotation of excited molecules thermalized. Implications for developing operational algorithms for massive processing of PFS and other instrument limb observations are discussed.

## 1 Introduction

For more than six Martian years the Planetary Fourier Spectrometer (PFS) on board the Mars Express satellite (Formisano et al., 2005) has been measuring the near-infrared radiances in both, nadir and limb geometries. For the study of Martian middle and upper (60-130 km) atmosphere limb measurements of the CO<sub>2</sub> 4.3 μm emission are of particular interest as the source of information on density and thermal structure of this layer. These measurements are achieved by the PFS' short wavelength channel (SWC) [1.25–5 μm] with the spectral resolution allowing to unambiguously identify many of the CO<sub>2</sub> emission bands. Details on the instrument description, its calibration and in-flight performance can be found in (Formisano et al., 2005; Giuranna et al., 2005; Formisano et al., 2006).

The strong daytime CO<sub>2</sub> 4.3 μm emission measured by PFS SWC are formed in the non-local thermodynamic equilibrium (non-LTE), which requires detailed accounting for the variety of processes influencing the ro-vibrational populations. The

excitation of the  $\text{CO}_2(\nu_3)$  vibrations is facilitated by absorption of solar radiation in the range of  $1 - 2.7 \mu\text{m}$  by the  $\text{CO}_2$  molecules. This excitation is followed by the cascade radiative one-quantum  $4.3 \mu\text{m}$  transitions, which escaping the atmosphere form the daytime atmospheric emission around  $4.3 \mu\text{m}$ . In addition, the collisional quenching of molecular vibrations (V-T processes) and the inter- and intra-molecular exchange of vibrational energy (V-V processes) also strongly influence the populations.

A number of studies (López-Valverde et al., 2005; Formisano et al., 2006; López-Valverde et al., 2011) (hereafter “previous studies”) were undertaken in recent years aimed at interpretation of the PFS SWC limb spectra. These studies consider only vibrational non-LTE in  $\text{CO}_2$  assuming molecular rotations completely thermalized (rotational LTE), and reiterate main features of daytime  $4.3 \mu\text{m}$   $\text{CO}_2$  emission formation in the upper atmosphere, which is dominated by the second hot (SH) and third hot (TH) bands of the main  $\text{CO}_2$  isotopologue (hereafter 626). Despite the good general understanding of how the absorption of solar radiation and subsequent redistribution of vibrational energy generate the hot  $\text{CO}_2$  band emissions, significant features present in the measured PFS spectra remain unexplained. Specifically, the majority of the daytime limb radiance measurements above approximately 90 km exhibit substantially stronger emissions than predicted by the non-LTE models in the spectral ranges  $2290\text{-}2305 \text{ cm}^{-1}$  and  $2345\text{-}2355 \text{ cm}^{-1}$  relative to the maxima of radiation at  $2317 \text{ cm}^{-1}$  and  $2335 \text{ cm}^{-1}$ , respectively (López-Valverde et al., 2011). An approach to explain this feature used in the previous studies was to treat the collisional rate coefficients as free parameters. However, the desired result was not reached, and it was speculated that remaining discrepancies might be due to contributions of some unidentified weak  $\text{CO}_2$   $4.3 \mu\text{m}$  bands not yet present in the HITRAN/HITEMP and GEISA spectroscopic databases. This issue remains unresolved until now. It prevents the science community to apply suitable retrieval algorithms for obtaining parameters of the Martian middle atmosphere from the PFS SWC limb spectra around  $4.3 \mu\text{m}$ .

In this paper we address this long standing discrepancy and provide its clear physical explanation.

## 2 Modeling the $4.3 \mu\text{m}$ emissions

### 2.1 The ALI-ARMS code

In this paper the  $\text{CO}_2$  non-LTE populations and limb spectra are calculated using the ALI-ARMS (for Accelerated Lambda Iterations for Atmospheric Radiation and Molecular Spectra) non-LTE code package (Kutepov et al., 1998; Gusev and Kutepov, 2003; Feofilov and Kutepov, 2012). ALI-ARMS utilizes the accelerated lambda iteration (ALI) technique developed in stellar astrophysics (Werner, 1986, 1987; Rybicki and Hummer, 1991; Pauldrach et al., 1994, 2001; Pauldrach, 2003; Hubeny and Lanz, 2003) for calculating the non-LTE populations of a very large number of atomic and ionic levels in optically thick atmospheres. ALI has become a standard technique for spectrum formation calculations and for the computation of the non-LTE model stellar atmospheres. The ALI-ARMS code has been successfully applied to the diagnostics of a number of space infrared Earth’s and Martian observations, both spectrally resolved (Kaufmann et al., 2002; Kaufmann et al., 2003; Maguire et al., 2002; Gusev et al., 2006) and broadband signals (Kutepov et al., 2006; Feofilov et al., 2009, 2012; Rezac et al., 2015), as well as to study the infra-red radiative cooling/heating in planetary atmospheres (Hartogh et al., 2005; Kutepov et al., 2007; Feofilov and Kutepov, 2012).

## 2.2 Rotational LTE and non-LTE

In order to establish a nominal result for a pure vibrational non-LTE model (complete rotational LTE is assumed) as used in previous studies we run ALI-ARMS for our extended reference CO<sub>2</sub> model for a dust-free atmospheric model retrieved from the Mars Climate Database (hereafter MCD)<sup>1</sup>, which matches the observation conditions. This reference model accounts for 150 vibrational levels of 5 CO<sub>2</sub> isotopologues and about 40k lines in calculating the non-LTE populations. The radiative transfer and solar absorption terms are calculated for all the 376 bands present in the task. We apply the same collisional rate coefficients for the lower vibrational levels as those used in previous studies, however, a different scaling of these basic rates for higher vibrational levels is performed based on the first-order perturbation theory as suggested by Shved et al. (1998).

Once the CO<sub>2</sub> populations are known we simulate the limb spectra in the range 2200 - 2400 cm<sup>-1</sup> for different tangent altitudes both with and without accounting for the overlapping, and compare them to the PFS observations. In our model we include in total 60 bands of the 5 isotopologues that contribute to the CO<sub>2</sub> 4.3 μm limb emission.

A random sample of the PFS measured spectrum is shown as a black curve in Fig.1. This and other spectra have been kindly provided for this study by the PFS PI M. Giuranna. The shown spectrum is an average of 27 single scans taken for the following conditions:  $L_s = 254$ , latitude = -67°, local time = 18 h, and solar zenith angle (SZA) = 69°, and tangent height of 115 km. As we already noted the effect addressed here is present in the majority of daytime spectra, therefore, no special criteria in latitude/longitude or local-time were applied to select these particular spectra for comparison with calculations here. The turquoise curve in Fig.1 presents the spectrum for our nominal run (these and other simulated spectra in this figure were obtained for SZA=69°). We show here the synthetic radiance for tangent height of 120 km since for a given input atmospheric model it provides better agreement with measured spectrum at 115 km.<sup>2</sup> Comparison in Fig.1 of simulated and measured signals obviously confirms the general conclusion of previous studies, i.e. above the altitude of 90 km, no matter the location and local time, *taking into account all known weak bands of CO<sub>2</sub> does not improve the mismatch* with the observed radiance in the “shoulders” (2290-2305 cm<sup>-1</sup> and 2345-2355 cm<sup>-1</sup>) relative to the maximum at 2317 cm<sup>-1</sup> and 2335 cm<sup>-1</sup>.

The problem of “incorrect” radiance distribution between cores and wings of molecular bands is not a new one and has been theoretically investigated in a series of papers by Kutepov et al. (1985); Ogibalov and Kutepov (1989); Kutepov et al. (1991) for CO<sub>2</sub> bands for atmospheric conditions of Mars and Venus, and for CO bands by Kutepov et al. (1997) for the Earth’s atmosphere. In these studies it has been shown that in the Martian atmosphere the Boltzmann rotational distribution for CO<sub>2</sub> molecules in the  $\nu_3$ -vibrationally excited states brakes down for altitudes above 80 km. At these altitudes the lifetime  $\tau = 1/A$  of these vibrational levels, where  $A \sim 200 \text{ s}^{-1}$  is the Einstein coefficient for the spontaneous 4.3 μm transitions, is not long enough for collisions to keep the rotation of excited molecules thermalized. Therefore, the need for complete vibrational-rotational non-LTE consideration has been identified already at that time.

<sup>1</sup><http://www-mars.lmd.jussieu.fr/mars/access.html>

<sup>2</sup>The mismatch of emission absolute values between measured and simulated spectra for the tangent altitude of 115 km (see also orange curve in Fig.1, discussed below) may be attributed both to the mismatch of input model and to the simplifying assumptions applied in this and previous studies, namely, the missing field-of-view averaging.

In this study we relax the assumption of rotational LTE for two vibrational levels 10011 and 10012 (HITRAN notation) of main CO<sub>2</sub> isotope 626. These levels are strongly pumped by the absorption of solar radiation at 2.7 μm and give origin to the two strong SH bands, which dominate the 4.3 μm limb emissions (Gilli et al., 2009; López-Valverde et al., 2011) of the Martian middle and upper atmosphere discussed here. We accounted for rotational sub-levels up to  $j = 102$  for each of these vibrational levels. The state-to-state rate coefficients describing rotational relaxation of vibrationally excited CO<sub>2</sub> were calculated as described by Kutepov et al. (1985) who applied the model of Preston and Pack (1977) and Pack (1979) based on infinite order sudden (IOS) approximation results. The total rotational relaxation rate used in these calculations was estimated as  $k_{rot}(T) = 2\pi k(T/p)\Delta\nu_L(T_o)(T/T_o)^{0.7}$ , where  $\Delta\nu_L$  is the Lorentz line width. The validity of this approach is discussed in detail for linear and non-linear molecules by Hartmann et al. (2008). For our model we used mean Lorentz width  $\Delta\nu_L$  of CO<sub>2</sub> rotational-vibrational lines from HITRAN12 (Rothman et al., 2013). With accounting for temperature dependence of these widths  $k_{rot} \approx 3 \times 10^{-10} \text{ cm}^3\text{sec}^{-1}$  for T =200 K.

### 3 Results and Discussion

#### 3.1 Importance of rotational non-LTE

The green curve in Fig.1 shows the spectrum calculated with accounting for the rotational non-LTE at vibrational levels 10011 and 10012 of main CO<sub>2</sub> isotope. One may see that this spectrum shows the redistribution of the radiances from SH band branch cores into there wings and, as a result, reproduces the measured signal shape significantly better than calculations based on the assumption of rotational LTE (turquoise curve).

**The reason for this alteration lies in the production of excited 626 molecules in vibrational states 10011 and 10012 due to the absorption of the 2.7 μm radiation in the altitude region of 80-140 km. In Figure 2 (left panel) we show this production rates, normalized over the rotational quantum number  $j$ , for state 10011 at the altitude of 120 km for SZA=69° (red), which correspond to simulated spectra presented in Fig. 1. Additionally, same pumping rates at 100 km for SZA=60° and 80° (green and blue, respectively) are shown for comparison.** Similar production rates was also obtained for level 10012. In general the molecules in level 10011 are most efficiently generated at the altitude of 120 km in rotational states with  $j = 25-40$  (30-50 for altitude of 100 km). The low production for  $j < 30$  is caused by a strong absorption of solar radiance in the cores of the 2.7 μm band branches in the upper atmosphere, which, however, remain transparent in the branch wings. At the altitudes above 90 km the collisions are not able to completely restore the Boltzmann rotational distribution of molecules in the vibrational states 10011 and 10012, and the latter takes form shown in the right panel of Fig.2. Compared to the Boltzmann distribution (read with circles) rotational non-LTE curve (red) demonstrates enhanced tail for  $j > 30$ , which reflects intensive radiative pumping of these levels shown in the left panel. Same is also true for two other curves (green and blue) shown in this panel for altitude 100 km. Latter demonstrate obvious dependence of the rotational LTE distortion on the SZA in agreement with corresponding production rate variation shown in the right panel of this figure.

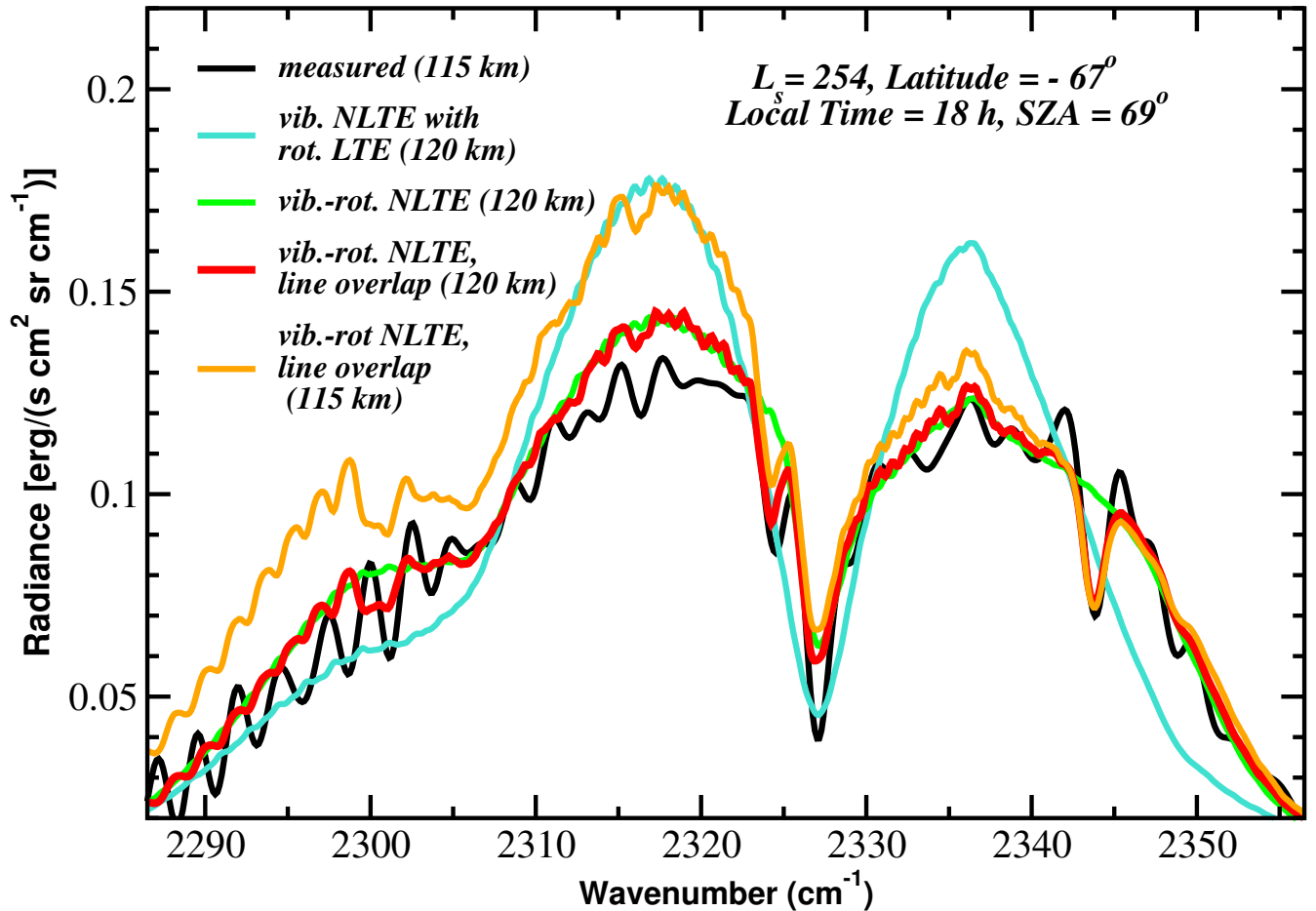


**Figure 1.** Comparison of measured (black) and simulated PFS SWC spectra. The observed spectrum is an average of 27 single scans taken for the following conditions:  $L_s = 254$ , latitude =  $-67^\circ$ , local time = 18 h, SZA =  $69^\circ$ , and tangent height of 115 km. The one sigma random uncertainties for this measured spectrum are shown. The simulated spectra are shown for tangent height of 120 km including only vibrational non-LTE in  $\text{CO}_2$  (turquoise), with vibrational-rotational non-LTE (green), and with vibrational-rotational non-LTE plus line overlapping along the line-of-sight (red). The spectra shown in orange color are calculated with same assumptions as for red, but for tangent height 115 km as a demonstration. (see text for detailed description)

### 3.2 Importance of line overlapping along the limb LOS

The rotational non-LTE spectrum in Fig.1 (green curve) reproduces general shape of measured signal (black curve) significantly better compared to that calculated with the rotational LTE assumption (turquoise curve). However, there are a number of small and medium size spectral features visible in the measured spectrum not present in the simulated one (green curve). So far

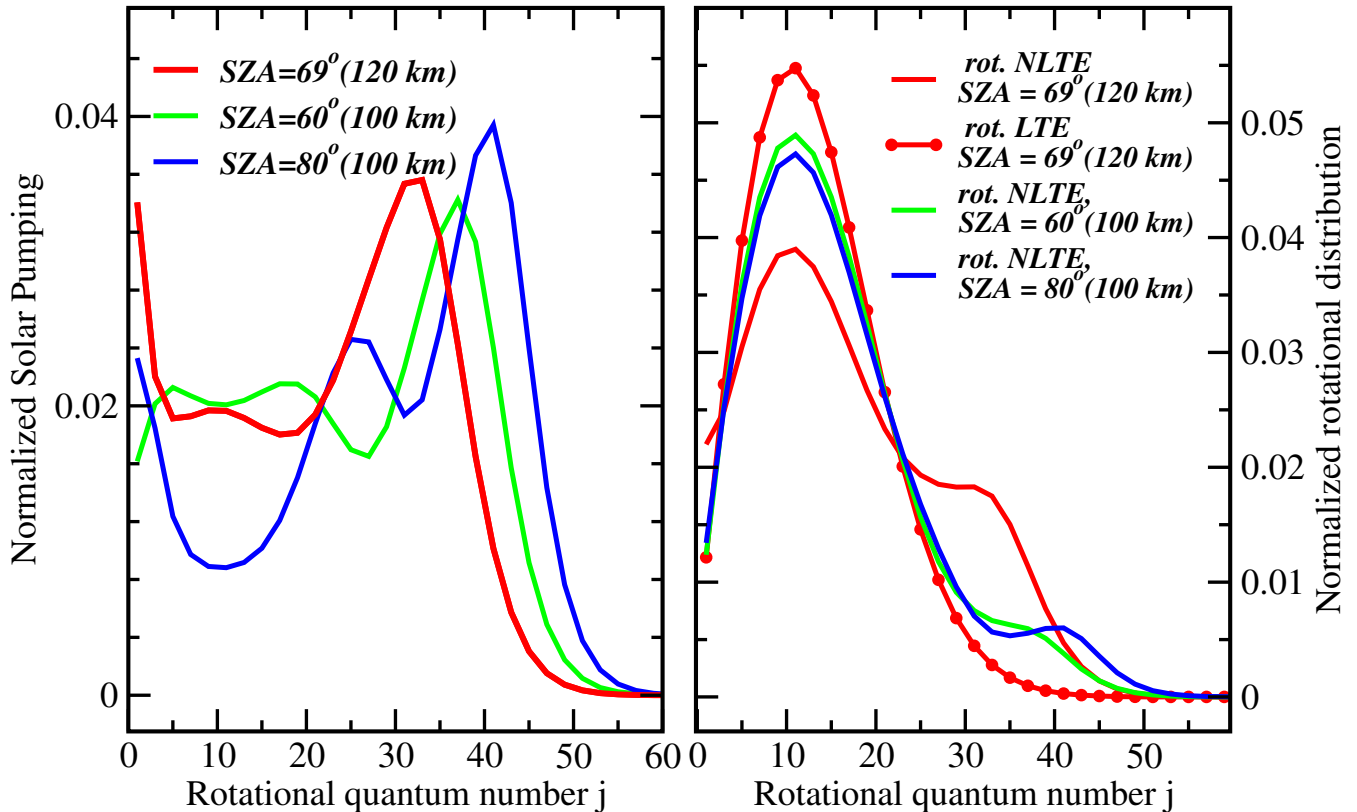


**Figure 2.** Left - normalized distribution of radiative pumping at level 10011 of  $^{12}\text{C}^{16}\text{O}_2$  due to the absorption of the  $2.7 \mu\text{m}$  solar radiation for altitudes of 100 and 120 km. Right - normalized rotational distribution at level 10011 of  $^{12}\text{C}^{16}\text{O}_2$  for altitudes of 100 and 120 km.

the synthetic spectra discussed here were calculated ignoring line overlapping along the LOS.<sup>3</sup> In this study we employed our radiance model in both, non-overlapping, and overlapping mode. In the latter case the calculations treat spectral line overlapping of all bands (within a band and between lines of different bands) of all isotopes in the line-by-line (LBL) fashion (technical discussion is detailed in Rezac et al. (2015)). The effect of accounting for line overlapping is clearly demonstrated in spectrum plotted in red color. Two well developed absorption features appeared, one around  $2344 \text{ cm}^{-1}$  and another one around  $2324 \text{ cm}^{-1}$ , which overlay well the corresponding features of measured spectrum. We found that the first of these features is caused by the absorption of radiation, which is emitted in the line R22e (here and below the line notations are taken from HITRAN) of the main isotope 10012-10002 SH band, by the nearly coincidental line R16e, which belongs to the fundamental band of isotope 628. Same is also true for the feature at  $2324 \text{ cm}^{-1}$ : here the emission line P4e of the 626 SH band 10012-10002 is blanketed by the line P15e of the first hot band 01111-01101 of same isotope.

<sup>3</sup> We note here also that although, previous studies report using forward model capable of treating line overlapping in limb calculations, its effects on PFS spectra were not discussed.

In addition, the “rotational non-LTE + overlapping on limb” spectrum (red curve) has an absorption feature around  $2316\text{ cm}^{-1}$ , which is, however, much less pronounced than the one in the measured spectrum. The formation mechanism of this signature is rather complex. Here, the emission line, R9e, belonging to the 10011-10001 SH band of the 628 isotope ( pumped by the  $2.7\text{ }\mu\text{m}$  solar radiation), is attenuated by the two nearby lines Q31f, and Q74f, from the 628 and 626 FH bands, respectively. To a smaller degree, several other lines located very closely to the R9e and belonging to various isotopic bands may also contribute this absorption signature. It should be noted that none of the vibrational levels of bands whose lines are involved in the formation of this absorption feature were treated accounting for the rotational non-LTE in this study. In general, rotational non-LTE at the lower vibrational level can influence the band absorption, whereas at the upper level the band emission is impacted. To get a better agreement with the measured spectrum, regarding the said absorption feature, as well as in the region  $2285\text{-}2305\text{ cm}^{-1}$ , where the synthetic spectrum does not reproduce a number of fine “wavy” features, we plan (a) to apply more detailed rotational non-LTE model, and (b) to use the exact procedure of spectra convolution, such as the “zeropadding”, as applied to the PFS interferograms (Giuranna et al., 2005). This signal processing technique certainly contributes to the formation of these “wavy” features of measured spectra.

#### 4 Conclusions

We present our first modeling results of the Mars Express PFS SWC daytime limb  $4.3\text{ }\mu\text{m}$  spectra for the altitude region above 90 km. We show that the long standing discrepancy between observed and calculated spectra in the cores and wings of the  $4.3\text{ }\mu\text{m}$  region is explained by the non-thermal rotational distribution of the  $^{12}\text{C}^{16}\text{O}_2$  molecules in upper vibrational levels 10011 and 10012 of the strong SH bands. The enhancement of the SH band wing emissions is caused (a) by intensive production of the  $\text{CO}_2$  molecules in rotational states with  $j > 30$  due to the absorption of solar radiation in optically thin wings of  $2.7\text{ }\mu\text{m}$  bands, and (b) by a short radiative life time of molecules in these states, which is insufficient at altitudes above 90 km for collisions to maintain rotation of excited molecules thermalized. As a results redistribution of SH band intensities takes place going from band branch cores into their wings. This result confirms significant impact of rotational non-LTE on the  $\text{CO}_2$   $4.3\text{ }\mu\text{m}$  emissions of Martian and Venusian atmospheres, which was predicted by Kutepov et al. (1985); Ogibalov and Kutepov (1989). *The PFS spectra provide the first strong evidence of this effect.*

Although, the rotational non-LTE on the levels 10011 and 10012 does an excellent job explaining the radiance redistribution observed in the measured spectra, more detailed simulations are still needed to investigate if there are smaller order effects caused by the rotational non-LTE at other  $\text{CO}_2$  vibrational levels. However, accounting for rotational non-LTE significantly slows down the non-LTE calculations, by an order of magnitude for the problem discussed in this paper.

Additional improvement in matching the  $4.3\text{ }\mu\text{m}$  band shape/structure between simulated and PFS measured spectra was reached by accounting for spectral line overlapping (within each band and among lines of different bands) along the limb LOS. This allowed to reproduce some fine absorption features in measured spectra that were missing in previous calculations, caused, however, factor of 10 increase of the limb emission computing time. **This additional computing time increase indicates the**

**need of significant efforts aimed at optimizing the rotational non-LTE/line overlapping simulation of PFS spectra to allow massive processing of measured PFS spectra.**

The presented results are also important for diagnostics of other similar observations. For instance, the Venus Express VIRTIS spectra around  $4.3 \mu\text{m}$  for tangent heights above 100-110 km, which are discussed in Gilli et al. (2009); López-Valverde et al. (2011), demonstrate remarkable resemblance of Mars Express PFS spectra analyzed in this study. Due to a well known similarity of the  $\text{CO}_2$  daytime emission formation mechanisms for both planets (Ogibalov and Kutepov, 1989) the Venus spectra obviously require also detailed rotational non-LTE/line overlapping analysis. These results may also be relevant for the analysis of limb mode measurements of the Trace Gas Orbiter/NOMAD instrument, which will start science operation in late 2017.

At last, we note that, as in previous studies, the following simplifications were applied in our simulations: (a) infinite-narrow FOV approximation was used, and (b) detailed spectra convolution was not performed, only simple ( $1 \text{ cm}^{-1}$ )-triangle window (to match the instrument spectral resolution) averaging of monochromatic spectra calculated on a fine grid was applied. Neither of these, however, influence the main results of this study. Nevertheless, missing FOV averaging (in combination with in-sufficient matching of applied pressure/temperature model) may explain better agreement (see Fig.1) between absolute emission values of spectrum measured for the tangent altitude of 115 km and that simulated for 120 km (compare black, red and orange line in this figure). Additionally, simplified averaging of monochromatic spectra in combination with missing FOV averaging may cause certain fine structure inconsistencies between measured and simulated spectra compared in this study.

*Acknowledgements.* The authors cordially thank Marco Giuranna, the PI of PFS/MEX, for providing us samples of PFS limb spectra with the emission features unexplained by the nominal non-LTE models, and for a very helpful discussion on the data quality, and the general performance of the instrument.

## References

- Feofilov, A. G. and Kutepov, A. A.: Infrared Radiation in the Mesosphere and Lower Thermosphere: Energetic Effects and Remote Sensing, *Surv. Geophys.*, 33, 1231–1280, doi:10.1007/s10712-012-9204-0, 2012.
- 5 Feofilov, A. G., Kutepov, A. A., Pesnell, W. D., Goldberg, R. A., Marshall, B. T., Gordley, L. L., García-Comas, M., López-Puertas, M., Manuilova, R. O., Yankovsky, V. A., Petelina, S. V., and Russell III, J. M.: Daytime SABER/TIMED observations of water vapor in the mesosphere: retrieval approach and first results, *Atmos. Chem. Phys.*, 9, 13 943–13 997, 2009.
- Feofilov, A. G., Kutepov, A. A., Rezac, L., and Smith, M. D.: Extending MGS-TES temperature retrievals in the martian atmosphere up to 90 km: Retrieval approach and results, *Icarus*, 221, 949–959, 2012.
- Formisano, V., Angrilli, F., Arnold, G., Atreya, S., Bianchini, G., Biondi, D., Blanco, A., Blecka, M. I., Coradini, A., Colangeli, L., 10 Ekonomov, A., Esposito, F., Fonti, S., Giuranna, M., Grassi, D., Gnedykh, V., Grigoriev, A., Hansen, G., Hirsh, H., Khatuntsev, I., Kiselev, A., Ignatiev, N., Jurewicz, A., Lellouch, E., Lopez Moreno, J., Marten, A., Mattana, A., Maturilli, A., Mencarelli, E., Michalska, M., Moroz, V., Moshkin, B., Nespoli, F., Nikolsky, Y., Orfei, R., Orleanski, P., Orofino, V., Palomba, E., Patsaev, D., Piccioni, G., Rataj, M., Rodrigo, R., Rodriguez, J., Rossi, M., Saggin, B., Titov, D., and Zasova, L.: The Planetary Fourier Spectrometer (PFS) onboard the European Mars Express mission, *Planet. Space Sci.*, 53, 963–974, doi:10.1016/j.pss.2004.12.006, 2005.
- 15 Formisano, V., Maturilli, A., Giuranna, M., D-Aversa, E., and López-Valverde, M.: Observations of non-LTE emission at 4-5 microns with the planetary Fourier spectrometer aboard the Mars Express mission, *Icarus*, 182, 51–67, 2006.
- Gilli, G., López-Valverde, M. A., Drossart, P., Piccioni, G., Erard, S., and Cardesín Moinelo, A.: Limb observations of CO<sub>2</sub> and CO non-LTE emissions in the Venus atmosphere by VIRTIS/Venus Express, *J. of Geophys. Res. (Planets)*, 114, E00B29, doi:10.1029/2008JE003112, 2009.
- 20 Giuranna, M., Formisano, V., Biondi, D., Ekonomov, A., Fonti, S., Grassi, D., Hirsch, H., Khatuntsev, I., Ignatiev, N., Michalska, M., Mattana, A., Maturilli, A., Moshkin, B. E., Mencarelli, E., Nespoli, F., Orfei, R., Orleanski, P., Piccioni, G., Rataj, M., Saggin, B., and Zasova, L.: Calibration of the Planetary Fourier Spectrometer short wavelength channel, *Planet. Space Sci.*, 53, 975–991, doi:10.1016/j.pss.2004.12.007, 2005.
- Gusev, O., Kaufmann, M., Grossmann, K., Schmidlin, F., and Shepherd, M.: Atmospheric neutral temperature distribution at the mesopause 25 altitude, *J. Atmos. and Solar-Terr. Physics*, 68, 1684–1697, 2006.
- Gusev, O. A. and Kutepov, A. A.: Non-LTE Gas in Planetary Atmospheres, in: *Stellar Atmosphere Modeling*, edited by Hubeny, I., Mihalas, D., and Werner, K., vol. 288 of *Astronomical Society of the Pacific Conference Series*, p. 318, 2003.
- Hartmann, J. M., Boulet, C., and Robert, D.: *Collisional Effects on Molecular Spectra*, Elsevier, 2008.
- Hartogh, P., Medvedev, A. S., Kuroda, T., Saito, R., Villanueva, G., Feofilov, A. G., Kutepov, A. A., and Berger, U.: Description and 30 climatology of a new general circulation model of the Martian atmosphere, *J. of Geophys. Res. (Planets)*, 110, E11 008, 2005.
- Hubeny, I. and Lanz, T.: Model Photospheres with Accelerated Lambda Iteration, in: *Stellar Atmosphere Modeling*, edited by Hubeny, I., Mihalas, D., and Werner, K., vol. 288 of *Astronomical Society of the Pacific Conference Series*, p. 51, 2003.
- Kaufmann, M., Gusev, O. A., Grossmann, K. U., Roble, R. G., Hagan, M. E., Hartsough, C., and Kutepov, A. A.: The vertical and horizontal distribution of CO<sub>2</sub> densities in the upper mesosphere and lower thermosphere as measured by CRISTA., *J. Geophys. Res.*, 107, 8182, 35 doi:10.1029/2001JD000704, 2002.

- Kaufmann, M., Gusev, O. A., Grossmann, K. U., Martín-Torres, F. J., Marsh, D. R., and Kutepov, A. A.: Satellite observations of daytime and nighttime ozone in the mesosphere and lower thermosphere, *J. of Geophys. Res. (Atmospheres)*, 108, 4272, doi:10.1029/2002JD002800, 2003.
- Kutepov, A. A., Hummer, D. G., and Moore, C. B.: Rotational relaxation of the  $00^0_1$  level of  $\text{CO}_2$  including radiative transfer in the  $4.3\mu\text{m}$  band of planetary atmospheres, *J. Quant. Spectrosc. Rad. Transfer*, 34, 101–114, 1985.
- Kutepov, A. A., Kunze, D., Hummer, D. G., and Rybicki, G. B.: The solution of radiative transfer problems in molecular bands without the LTE assumption by accelerated lambda iteration methods, *J. Quant. Spectrosc. Rad. Transfer*, 46, 347–365, doi:10.1016/0022-4073(91)90038-R, 1991.
- Kutepov, A. A., Oelhaf, H., and Fischer, H.: Non-LTE radiative transfer in the  $4.7$  and  $2.3\mu\text{m}$  bands of  $\text{CO}$ : vibration-rotational non-LTE and its effects on limb radiance., *J. Quant. Spectrosc. Rad. Transfer*, 57, 317–339, doi:10.1016/S0022-4073(96)00142-2, 1997.
- Kutepov, A. A., Gusev, O. A., and Ogibalov, V. P.: Solution of the Non-LTE Problem for Molecular Gas in Planetary Atmospheres: Superiority of Accelerated Lambda Iteration, *J. Quant. Spectrosc. Rad. Transfer*, 60, 199–220, 1998.
- Kutepov, A. A., Feofilov, A. G., Marshall, B. T., Gordley, L. L., Pesnell, W. D., Goldberg, R. A., and Russell, J. M.: SABER temperature observations in the summer polar mesosphere and lower thermosphere: Importance of accounting for the  $\text{CO}_2$   $\nu_2$  quanta V-V exchange, *Geophys. Res. Lett.*, 33, L21809, doi:10.1029/2006GL026591, 2006.
- Kutepov, A. A., Feofilov, A. G., Medvedev, A. S., Pauldrach, A. W. A., and Hartogh, P.: Small-scale temperature fluctuations associated with gravity waves cause additional radiative cooling of mesopause the region, *Geophys. Res. Lett.*, 34, L24 807, 2007.
- López-Valverde, M., López-Puertas, M., López-Moreno, J. J., Formisano, V., Grassi, D., Maturilli, A., Lellouch, E., and Drossart, P.: Analysis of  $\text{CO}_2$  non-LTE emissions at  $4.3\mu\text{m}$  in the Martian atmosphere as observed by PFS/Mars Express and SWS/ISO, *Planet. Space Sci.*, 53, 1079–1087, 2005.
- López-Valverde, M. A., López-Puertas, M., Funke, B., Gilli, G., Garcia-Comas, M., Drossart, P., Piccioni, G., and Formisano, V.: Modeling the atmospheric limb emission of  $\text{CO}_2$  at  $4.3\mu\text{m}$  in the terrestrial planets, *Planet. Space Sci.*, 59, 988–998, doi:10.1016/j.pss.2010.02.001, 2011.
- López-Valverde, M. A., Sonnabend, G., Sornig, M., and Kroetz, P.: Modelling the atmospheric  $\text{CO}_2$   $10\text{-}\mu\text{m}$  non-thermal emission in Mars and Venus at high spectral resolution, *Planet. Space Sci.*, 59, 99–1009, doi:10.1016/j.pss.2010.11.011, 2011.
- Maguire, W. C., Pearl, J. C., Smith, M. D., Conrath, J., Kutepov, A. A., Kaelberer, M. S., Winter, E., and Christensen, P. R.: Observations of high-altitude  $\text{CO}_2$  hot bands in Mars by the orbiting Thermal Emission Spectrometer, *Geophys. Res. Lett.*, 127, 5063, 2002.
- Ogibalov, V. P. and Kutepov, A. A.: An approximate solution for radiative transfer in the  $4.3\mu\text{m}$   $\text{CO}_2$  band: thick atmosphere with breakdown of rotational LTE, *Sov. Astron.*, 33, 511–519, 1989.
- Pack, R. T.: Pressure broadening of the dipole and Raman lines of  $\text{CO}_2$  by He and Ar. Temperature dependence, *J. Chem. Phys.*, 70, 3424–3433, doi:10.1063/1.437876, 1979.
- Pauldrach, A. W. A.: Hot Stars: Old-Fashioned or Trendy? (With 24 Figures), in: *Reviews in Modern Astronomy*, edited by Schielicke, R. E., vol. 16 of *Reviews in Modern Astronomy*, p. 133, 2003.
- Pauldrach, A. W. A., Kudritzki, R. P., Puls, J., Butler, K., and Hunsinger, J.: Radiation-driven winds of hot luminous stars. 12: A first step towards detailed UV-line diagnostics of O-stars, *A&A*, 283, 525–560, 1994.
- Pauldrach, A. W. A., Hoffmann, T. L., and Lennon, M.: Radiation-driven winds of hot luminous stars. XIII. A description of NLTE line blocking and blanketing towards realistic models for expanding atmospheres, *A&A*, 375, 161–195, doi:10.1051/0004-6361:20010805, 2001.

- Preston, R. K. and Pack, R. T.: Classical trajectory studies of rotational transitions in Ar-CO<sub>2</sub> collisions, *J. Chem. Phys.*, 66, 2480–2487, 1977.
- Rezac, L., Kutepov, A., Russell, J. M., Feofilov, A. G., Yue, J., and Goldberg, R. A.: Simultaneous retrieval of T(p) and CO<sub>2</sub> VMR from two-channel non-LTE limb radiances and application to daytime SABER/TIMED measurements, *J. Atmos. and Solar-Terr. Physics*, 130, 23–42, doi:10.1016/j.jastp.2015.05.004, 2015.
- Rothman, L., Gordon, I., Babikov, Y., Barbe, A., Benner, D. C., Bernath, P., Birk, M., Bizzocchi, L., Boudon, V., Brown, L., Campargue, A., Chance, K., Cohen, E., Coudert, L., Devi, V., Drouin, B., Fayt, A., Flaud, J.-M., Gamache, R., Harrison, J., Hartmann, J.-M., Hill, C., Hodges, J., Jacquemart, D., Jolly, A., Lamouroux, J., Roy, R. L., Li, G., Long, D., Lyulin, O., Mackie, C., Massie, S., Mikhailenko, S., Muller, H., Naumenko, O., Nikitin, A., Orphal, J., Perevalov, V., Perrin, A., Polovtseva, E., Richard, C., Smith, M., Starikova, E., Sung, K., Tashkun, S., Tennyson, J., Toon, G., Tyuterev, V., and Wagner, G.: The {HITRAN2012} molecular spectroscopic database, *J. Quant. Spectrosc. Rad. Transfer*, 130, 4 – 50, 2013.
- Rybicki, G. B. and Hummer, D. G.: An accelerated lambda iteration method for multilevel radiative transfer I. Non-overlapping lines with background continuum, *A&A*, 245, 171–181, 1991.
- Shved, G. M., Kutepov, A. A., and Ogibalov, V. P.: Non-local thermodynamic equilibrium in CO<sub>2</sub> in the middle atmosphere. I. Input data and populations of the  $\nu_3$  mode manifold states, *J. Atmos. and Solar-Terr. Physics*, 60, 289–314, 1998.
- Werner, K.: Construction of non-LTE model atmospheres using approximate lambda operators, *A&A*, 161, 177–182, 1986.
- Werner, K.: *Stellar Atmospheres in Non-LTE: Model Construction and Line Formation Calculations using Approximate Lambda Operators*, p. 67, Cambridge U. Press, 1987.